

Conversion of cellulose to short chain polyols over metal loaded on KCC-1 catalyst

F. Ariffin^a, S.M. Izan^a, A.A. Jalil^b, C.R. Mamat^a, N. Basar^a, J. Jaafar^a, H. Hamdan^c, S. Triwahyono^{a,*}

^aDepartment of Chemistry, Faculty of Science, Universiti Teknologi Malaysia, 81310 Johor Bahru, Malaysia

^bDepartment of Chemical Eng., Faculty of Chemical and Energy Eng., Universiti Teknologi Malaysia, 81310 Johor Bahru, Malaysia

^cUTM Razak School of Engineering and Advanced Technology, UTM Kuala Lumpur, Razak Tower, Jalan Sultan Yahya Petra, 54100 Kuala Lumpur, Malaysia

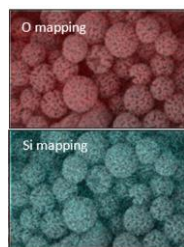
*Corresponding author email: sugeng@utm.my

Article history :

Received 30 May 2017

Accepted 25 August 2017

GRAPICAL ABSTRACT



EDX mapping of KCC-1

ABSTRACT

The production of short chain polyols from cellulose over metal (Ce, Ni or Ru) loaded on fibrous mesoporous silica KCC-1 catalysts was studied at temperature range of 150-240 °C. The KCC-1 was prepared by microwave assisted hydrothermal method. Then it was modified with Ce, Ni or Ru by incipient wetness impregnation method. The KCC-1, Ce/KCC-1, Ni/KCC-1 and Ru/KCC-1 were characterized with XRD, FESEM, FTIR and nitrogen-physorption analyzer. The XRD analysis showed that the introduction of metals did not change much of the XRD pattern for KCC-1. The FESEM and EDX results showed the presence of Ce, Ni and Ru metals on the uniform spherical shape of fibrous silica particle. The surface area of KCC-1, Ce/KCC-1, Ni/KCC-1 and Ru/KCC-1 was 393.81, 371.56, 314.22 and 351.97 m²/g, respectively. At 220 °C, 5 bars of nitrogen, and 2 h of reaction, the conversion of cellulose reached 95 % over Ce/KCC-1 with the product distribution of 3-buten-1-ol (S=63.30%), diisopropyl ether (S=2.86%) and cyclopropane carboxylic acid (S=33.70%). While, bare KCC-1, Ni/KCC-1 and Ru/KCC-1 showed less activity than that of Ce/KCC-1. The high activity of Ce/KCC-1 may be due to the presence of Ce metal and fibrous silica which provided large surface area and average pore diameter.

Keywords: Cellulose, Cerium, Ruthenium, Nickel, KCC-1

© 2017 Dept. of Chemistry, UTM. All rights reserved
| eISSN 0128-2581 |

1.0 INTRODUCTION

At this present time, the world is strongly dependent on the fossil fuels as a primary source of energy and its usage is very obvious in the industrialized country. In order to cater sufficient energy for the current and upcoming generation, another alternative need to be identified to replace the roles of fossil fuel. Cellulose is one of the most abundant sources of biomass and generally the good alternative for fossil fuel energy. The chemocatalytic cleavage of cellulose's C-C and C-O bonds into polyols through has attracted much attention because of its renewable and carbon-neutral properties [1,2]. However, cellulose has a highly crystalline structure and resistant microfibrils network with extensive intra and intermolecular hydrogen bonding. Due to these properties, cellulose is hard to be degraded in mild condition [3]. Further work is needed to explore this area especially the catalyst needed to degrade the cellulose [4] and the effective condition of reaction.

Extensive attention was paid to the direct conversion of cellulose to polyols over heterogeneous catalyst in hot-compressed water [5]. Fukuoka and Dhepe reported the first direct conversion of cellulose to hexitols on Pt/Al₂O₃ in water without the use of any mineral acids [2]. In addition, the use of transition metal catalysts was said to be active in assisting the production of cellulose to diols. Wang and

coworkers (2010) found that Ru as the most effective for the conversion of cellulose to sorbitol with CNT as the support.

In this study, cerium (Ce), nickel (Ni) and ruthenium (Ru) loaded on KCC-1 support have been examined in the conversion of cellulose into short chain polyols in high pressure autoclave apparatus. The study focused on the effect of gas pressure, reaction temperature and time.

2.0 EXPERIMENTAL

2.1 Preparation of KCC-1 and metal loaded on KCC-1

Fibrous mesostructured silica particle was prepared by the microwave assisted hydrothermal method. In brief, the procedure is as follows. Tetraethyl orthosilicate (TEOS, 2.5 g, 0.012 mol) was dissolved in a mixture of cyclohexane (30 mL) and pentanol (1.5 mL). Then, a mixture of cetylpyridinium bromide (CPB; 1 g, 0.0026 mol), urea (0.6g, 0.01 mol) and water (30 ml) was added. The mixture then stirred for 30 min at room temperature and the resulting solution was placed in a Teflon sealed autoclave reactor. The reaction mixture was exposed to intermittent MW irradiation (400W) for 4 h. Then, the solid product was isolated by centrifugation at 20,000 rpm, followed by washing with acetone and distilled water, and was dried overnight in air at 100 °C. Finally the product was calcined at 550 °C for 6 h under an air atmosphere to obtain KCC-1. The Ce/KCC-1, Ni/KCC-1

and Ru/KCC-1 were prepared by impregnation of Cerium (III) nitrate hexahydrate ($\text{Ce}(\text{NO}_3)_3 \cdot 6\text{H}_2\text{O}$), Nickel (II) nitrate hexahydrate ($\text{Ni}(\text{NO}_3)_2 \cdot 6\text{H}_2\text{O}$) and Ruthenium (III) nitrate hexahydrate ($\text{Ru}(\text{NO}_3)_3 \cdot 6\text{H}_2\text{O}$). The catalyst then dried and calcined at 550°C in air. The transition metal content (Ni, Ce, Ru,) was adjusted to be 5 wt%.

2.2 Catalysts characterization

XRD patterns were recorded with a Bruker AXS D8 Automatic Powder diffractometer using $\text{CuK}\alpha$ radiation. Field Emission Scanning Electron Microscope (FESEM) from JEOL JSM 6710 F with 15 kV used to identify the morphological features and surface characteristics of catalysts. The chemical element in the catalysts was determined by FESEM-EDX. The adsorption-desorption isotherm of N_2 at -196°C were obtained with Beckman Coulter SA 3100 Surface Area Analyzer apparatus after outgassing the samples at 300°C for 1 h. Fourier Transform Infra-Red (FTIR) measurements were performed at room temperature on an Agilent Cary 640 Series FTIR spectrometer equipped with a high-temperature stainless steel cell with CaF_2 windows provided with a heatable cell (up to 500°C) connected to a vacuum system and a gas manifold.

2.3 Conversion of cellulose to alcohol

The reaction was performed at $150\text{--}240^\circ\text{C}$ in a stainless-steel autoclave using N_2 gas (1-5 bar) as follow: the catalyst (0.05 g) and cellulose (0.324 g) were added in a mixture of 30 mL of water and 10 mL of isopropanol. The solution then stirred (1000 rpm) for 2h. The resulted reaction mixture was cooled. The bulk of catalyst removed by filtration and the liquid phase evaporated under vacuum at -100°C for 24 h.

The products were identified with gas chromatograph (GC, 7890A, Agilent, USA) coupled with a mass spectrometer (MS, 5975C, Agilent, USA). The gas chromatogram-mass spectrometer (GC-MS) was equipped with a HP-INNOWax column (30 m \times 0.25 mm; film thickness, 0.25 μm). The temperature of injection was at 250°C . Argon was used as the carrier gas, and its flow rate was 0.3 mL min^{-1} .

3.0 RESULTS AND DISCUSSION

3.1 X-Ray Diffraction analysis

XRD analysis was used to determine the crystalline structure and characterize the structure of catalysts calcined at high temperature. Fig. 1 illustrates the X-Ray Diffraction patterns of KCC-1, Ce/KCC-1, Ni/KCC-1 and Ru/KCC-1 catalysts. All catalysts showed worm-like SiO_2 pattern below $2\theta = 5^\circ$. The introduction of metal to the KCC-1 did not alter much the pattern of KCC-1. In addition, there is no absorption peaks exhibited the presence of crystalline metal for parent, Ni and Ce loaded on KCC-1 which may be due to the small

amount of metal content or below the detection limit XRD instrument. However small peaks were observed at $2\theta = 27^\circ$, 35° and 54° for Ru/KCC-1 which corresponding to Ru (202), (002) and (204), respectively [6].

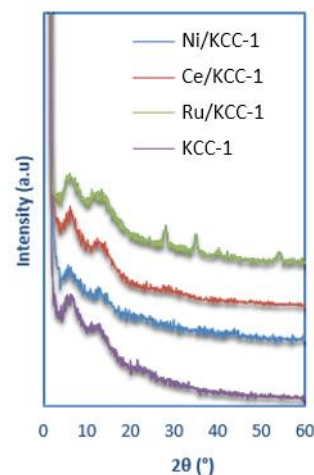


Fig. 1 XRD patterns of pure and modified KCC-1

3.2 Field Emission Scanning Electron Microscope

The morphology of KCC-1 is shown in the Fig. 2. KCC-1 possessed spherical shape of silica dendrimer network that widened disordered radially outward with particle size of 600-700 nm. The parent KCC-1 was only containing Si and O elements. The introduction of Ni, Ce and Ru did not much change the morphology and average particle size of KCC-1 (Fig. 3). The Elemental mapping showed widely distributed Si atoms and O atoms was mainly in the center of each sphere. While, Ce and Ni atom was scarcely distributed on the Ce/KCC-1 and Ni/KCC-1. For Ru atom, it was evenly distributed on the Ru/KCC-1.

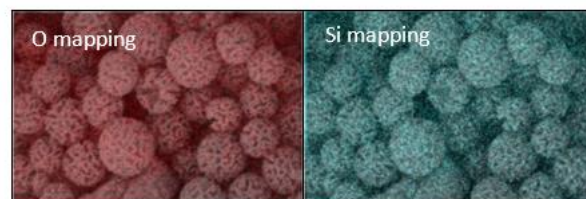


Fig. 2 FESEM and EDX mapping of KCC-1

3.3 N_2 physisorption analysis

The textural properties of all catalysts were characterized by using N_2 adsorption-desorption. Figure 4 illustrates the isotherms and pore distribution of all catalysts. All catalysts exhibited type IV isotherms with H_3 hysteresis loop, which are associated with mesoporous materials with various sizes of slit-shaped pores at low pressure showing the presence of microporous [7]. N_2 isotherms displayed high N_2 uptake at

high relative pressure (0.4-0.9) and parent KCC-1 showed highest N_2 uptake in the high relative pressure followed by Ce/KCC-1, Ni/KCC-1 and Ru/KCC-1 (Figure 4). This could be attributed to the high number of interparticle pore which may be come from the distance between silica dendrimer which are affected by the presence of the metal loading. The pore distribution was obtained by using non-local density functional theory (NLDFT). All catalysts exhibited pore size centered at 1.3, 3.1 and 4.6 nm which could be attributed to the self-assembly of micelle and inter-dendrimer distance, respectively [8-10]. Parent KCC-1 appeared to possess the largest pore at 4.6 nm followed by Ni/KCC-1, Ce/KCC-1 and Ru/KCC-1. No microporous was observed for parent KCC-1. The introduction of metal decreased porous at 4.6 nm and developed porous with size of 3.1 and 1.2 nm. The difference in the N_2 uptake and pore distribution of each catalyst is due to their difference in inter-dendrimer distance and the presence of metal loading. The difference of inter-dendrimer distance was also affecting the total pore volume and surface area of each catalyst, as shown in Table 1. The BET specific surface area of KCC-1 and metal (Ce, Ni and

Ru) loaded on KCC-1 are 394, 372, 314 and 352 m^2/g respectively. The total pore volume of KCC-1 decreased from 0.636 to 0.470, 0.431 and 0.376 cm^3/g after the introduction of Ce, Ni and Ru.

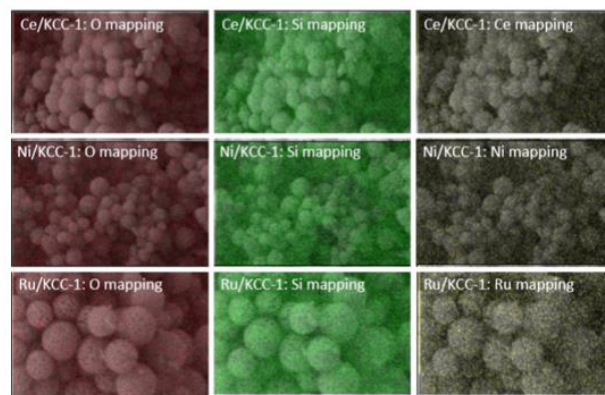


Fig. 3 FESEM images and elemental mappings for Ce/KCC-1, Ni/KCC-1 and Ru/KCC-1

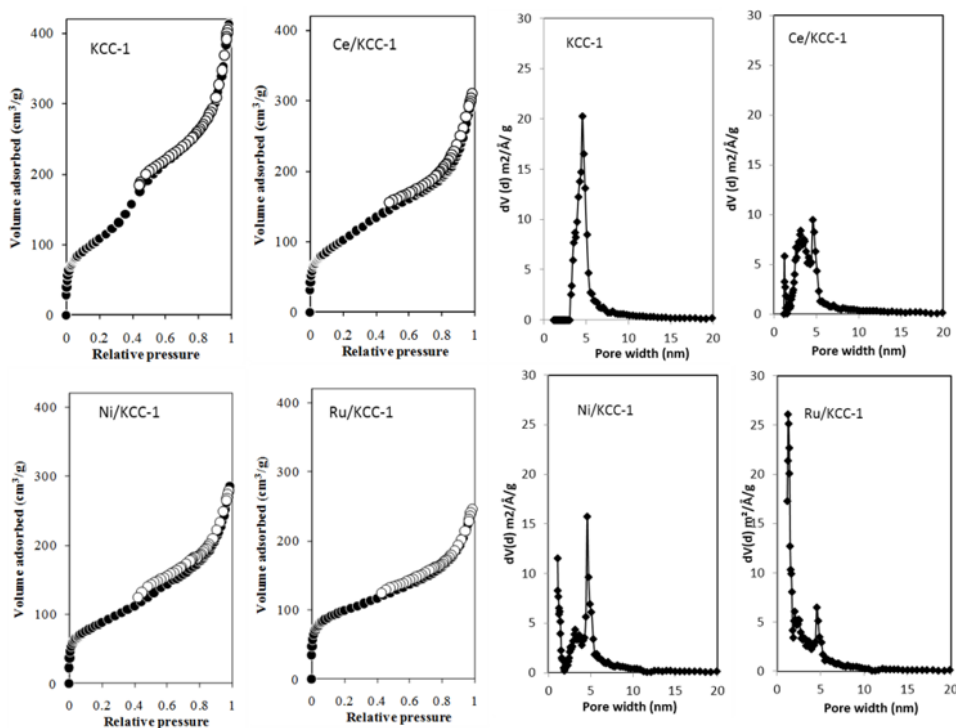


Fig. 4 N_2 adsorption-desorption isotherm and pore size distribution of KCC-1 and metal loaded on KCC-1

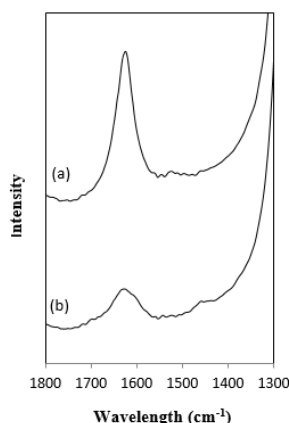
3.4 Nature of Basicity

Several probe molecules including carbon dioxide, ammonia, and pyridine were used to characterize the basicity of metal catalyst. In this study, CO_2 was used to determine the basicity of the catalyst. CO_2 is a probe for the basicity analysis of solids, as it forms carbonate-like species with basic oxygen atoms. In this study, in-situ FTIR spectra of adsorbed

CO_2 was used to illustrate the states of adsorbed CO_2 species that interacted with the basic sites on the surface of Ce/KCC-1 catalysts. From Figure 5 at the desorption temperature of $150^\circ C$, there are two prominent peaks were observed at 1631 and 1470 cm^{-1} , which are attributed to symmetric and asymmetric O-C-O stretching modes of bidentate carbonates, respectively.

Table 1 The surface area and pore volume of KCC-1 and metals (Ce, Ni and Ru) loaded on KCC-1.

| Catalyst | Surface Area (m ² /g) | Pore Volume (cm ³ /g) |
|----------|----------------------------------|----------------------------------|
| KCC-1 | 394 | 0.636 |
| Ce/KCC-1 | 372 | 0.470 |
| Ni/KCC-1 | 314 | 0.431 |
| Ru/KCC-1 | 352 | 0.376 |

**Fig. 5** CO₂ adsorbed IR of Ce/KCC-1 a) ads RT, b) des 150

3.5 Hydrogenolysis of cellulose

The hydrogenolysis of cellulose was conducted over KCC-1, Ce/KCC-1, Ni/KCC-1 and Ru/KCC-1 at $T = 150\text{ }^{\circ}\text{C}$, $H_2 = 1\text{ Bar}$, 0.05 g catalyst , 0.324 g cellulose , and $t = 1\text{ hr}$ unless otherwise specified. The conversion of cellulose is tabulated in the Table 2. The KCC-1 exhibited lowest conversion of cellulose compared to metal loaded on KCC-1 catalysts. The Ni/KCC-1 and Ru/KCC-1 resulted almost similar conversion of cellulose, while Ce/KCC-1 exhibited highest cellulose conversion of 16.0 %. The low cellulose conversion for KCC-1 may be due to the absence of metal active sites which required in the adsorption and dissection of hydrogen molecule to hydrogen atoms. The presence of Ni, Ru and Ce markedly increased the conversion of cellulose over KCC-1 catalyst.

Table 2 shows the effect loading metal, hydrogen pressure, reaction time and temperature in the cellulose conversion. It could be seen that as the hydrogen pressure increased the cellulose conversion was enhanced slightly. By increasing the hydrogen pressure, the volume of gas decreases and the collision between cellulose and gas particles are rapid, thus the chemical reaction proceeds [11]. However, the cellulose conversion was almost the same in the whole pressure range investigated. For the safety of the reaction situation, the optimum pressure was set to 5 bars since the conversion of cellulose is still in range as the high pressure and used in further optimization other parameters. As shown from the Table 2, the conversion of cellulose was promoted when the reaction temperature increased from 150-240 $^{\circ}\text{C}$. The maximum cellulose conversion can be obtained

at 220 $^{\circ}\text{C}$ or above. The in-situ generations of H^+ are more vigorous at high temperature and consequently assisted the process hydrolysis of cellulose [12]. However, at a very high temperature, the product might be decomposed and the catalyst tend to be deactivated [13], hence the optimum temperature was set to 220 $^{\circ}\text{C}$.

The activation energy obtained from the plot is 2669.29 Jmol⁻¹. As had been mentioned, the cellulose conversion reached up to 98.93% as the temperature increases which means that the activation energy was overcome by the high reaction temperature. Table 3 shows the effect of reaction time on the conversion of cellulose. It was clear that the conversion rate is strongly dependent on reaction time. When the reaction proceeded from 1h to 6 h, the cellulose conversion changed from 46.22% to 95%. The longer reaction time allowed the cellulose to interact with the catalyst and as well as the hydrogen gas. Therefore, the longer reaction time enhanced the conversion of cellulose.

3.6 Gas Chromatography Mass Spectroscopy

Products of hydrogenolysis of cellulose over Ce/KCC-1 investigated at different reaction temperatures. Table 4.6 shows the product distribution and selectivity of products obtained from the reaction as the temperature increased. It could be seen that, at lower temperature, the product obtained only 2-amino-1-propanol. The presence of amino group in the product suggests that the reaction is incomplete and the temperature is not enough to convert the cellulose into any other products.

The product distribution varied as the temperature of the reaction changed. As the temperature increase to 200 $^{\circ}\text{C}$, cyclopropane and diisopropyl ether was obtained and this could be due to the higher temperature that assists the cleavage of cellulose into alkane and ether. Ether could be converted to other short chain polyols by further hydrogenolysis process [14].

At the maximum temperature 220 $^{\circ}\text{C}$, the presence of 3-buten-1-ol proved that the diisopropyl ether can be further converted into polyols. However, cyclopropane carboxylic acid was also produced at higher temperature. The formation of carboxylic acid can be explained by the disproportionation of aldehyde [11]. It was reported that the ion product (K_w) of water at 250 $^{\circ}\text{C}$ is about 3 orders of magnitude higher than that of ambient temperature. This means that more concentration of H^+ produced at higher temperature. The dissolution and hydrolysis of cellulose will be accelerated as the concentration of H^+ increased. It is technically known that C-C hydrogenolysis reaction have high activation energy than hydrogenation. Thus the temperature increase logically favors the reaction with highest activation energy.

The ability of KCC-1 to disperse the metal Ce very well increased the catalytic activity and therefore utilize in the hydrogenolysis reaction. Moreover, the basic site of Ce metal assisted the cleavage of C-C bond in cellulose [12]. Hydrogenolysis of reaction conducted under those optimized parameters and the product obtained was analyzed by

using GCMS. Table 3 shows the product distribution and selectivity of each product at different temperature. The product distributions varied as the temperature of the reaction changed. As the temperature increase to 200°C, cyclopropane and diisopropyl ether were obtained and this could be due to the higher temperature that assists the cleavage of cellulose into alkane and ether. Ether could be converted to other short chain polyols by further hydrogenolysis process [2]. At the maximum temperature 220°C, the presence of 3-buten-1-ol proved that the diisopropyl ether can be further converted into polyols. However, cyclopropane carboxylic acid was also produced at higher temperature. The disproportionation of aldehyde into carboxylic acid may explained the formation of carboxylic acid product [5].

Table 2 Percentage of cellulose conversion with different catalysts

| Catalyst | Temperature [°C] | Pressure [Bar] | Time [h] | Conversion of cellulose (%) |
|----------|------------------|----------------|----------|-----------------------------|
| KCC-1 | 150 | 1 | 1 | 3.8 |
| Ru/KCC-1 | 150 | 1 | 1 | 13.6 |
| Ni/KCC-1 | 150 | 1 | 1 | 13.1 |
| Ce/KCC-1 | 150 | 1 | 1 | 16.3 |
| | 150 | 2.5 | 1 | 17.0 |
| | 150 | 5 | 1 | 24.9 |
| | 150 | 7.5 | 1 | 26.9 |
| | 150 | 10 | 1 | 28.2 |
| | 150 | 5 | 2 | 45.3 |
| | 180 | 5 | 2 | 70.5 |
| | 200 | 5 | 2 | 83.3 |
| | 220 | 5 | 2 | 95.0 |
| | 240 | 5 | 2 | 98.9 |
| | 150 | 5 | 3 | 68.6 |
| | 150 | 5 | 4 | 88.9 |
| | 150 | 5 | 5 | 95.30 |

Table 3 Product distributions and selectivity of product at different temperature

| Temperature(°C) | 150 | 200 | 220 |
|---------------------|------|--------|-------|
| Cyclopropane | - | 92.24% | - |
| Diisopropyl Ether | - | 7.74% | 2.86% |
| 3-buten-1-ol | - | - | 63.3% |
| 2-Amino-1-propanol | 100% | - | - |
| Cyclopropionic acid | - | - | 33.7% |

4. CONCLUSION

In summary, this study had demonstrated that KCC-1 supported Ce catalyst allows the high selectivity of short chain polyols from microcrystalline cellulose under H₂ in hot compressed water via hydrogenolysis process. The Ce/KCC-1 investigated could effectively catalyze the the one-pot conversion of microcrystalline cellulose and the supports played a critical role in the product distribution and selectivity. The best result obtained was at the temperature of 220°C with 95% of cellulose conversion and 63.3 % selectivity towards 3-buten-1-ol.

ACKNOWLEDGEMENTS

We are grateful for the support by the Nippon Sheet Glass Foundation for Materials Science and Engineering, Japan no. 4B181 and the Ministry of Higher Education Malaysia through “NanoMITE“ Long Term Research Grant Scheme no. 4L823.

REFERENCES

- [1] O. Roselinde, D. Michiel, A.G. Jan, B. Beau, V. Rick, G. Elena, A.M. Johan, R. Andreas, F.S. Bert, *Green Chem.* 16 (2014) 695.
- [2] W. Xicheng, M. Lingqian, W. Feng, J. Yijun, W. Lei, M. Xindong, *Green Chem.* 14 (2012) 758.
- [3] W. Yujing, Q. Songbai, X. Ying, D. Mingyue, C. Lungang, Z. Qi, M. Longlong, W. Tiejun, *Energy and Management* 94 (2015) 95.
- [4] K. Deutsch, Copper catalysts in the C-O hydrogenolysis of biorenewable compounds, Graduate Theses and Dissertations, 2012, 12312.
- [5] A. G. Jan, V.D.V. Stijn, O. Roselinde, O.D.B. Beau, A.J. Pierre, F.S. Bert, *Catal. Sci. Technol.* 1 (2012) 714.
- [6] K. Hirokazu, K. Tasuku, K.G. Samar, H. Kenji, F. Atsushi, *Appl. Catal. A: Gen.* (2011) 409.
- [7] L. Yuping, L. Yuhe, C. Xiaofeng, W. Tiejun, M. Longlong, L. Jinxing, L. Qiying, X. Ying, *Biomass Bioenergy.* 74 (2015) 148.
- [8] G. Jan, V.D.V. Stijn, C. Kevin, J. Pierre, S. Bert, *Green Chem.* 13 (2011) 2167.
- [9] V. Lea, C. Amandine, E. Catherine, L. Sylvie, D. Daniel, J. Catal. 320 (2014) 16.
- [10] S. Jinliang, F. Honglei, M. Jun, H. Buxing, *Green Chem.* 15 (2013) 2619.
- [11] X. Jinxu, Z. Yu, X. Qineng, L. Xiaohui, R. Jiawen, L. Guanzhong, W. Yanqin, *Appl. Catal. A: Gen.* 459 (2013) 52.
- [12] X. Jinxu, D. Daqian, S. Yi, L. Xiahui, L. Guanzhong, W. Yanqin, *Chem. Eng.* 2 (2014) 2355.
- [13] L. Mingrui, W. Hua, H. Jinyu, N. Yufei, *Carbohydr. Polym.* 89 (2012) 607.
- [14] M.L. Inmaculada, L.G. Manuel, L.G.F. Jose, M. Rafael, *Chin. J. Catal.* 35 (2014) 614.